Eocene arc-continent collision in northern Kamchatka, Russian Far East

Alexey V. Soloviev,[1] John I. Garver,[2] Mikhail N. Shapiro,[3] Mark T. Brandon,[4] and Jeremy K. Hourigan[5]

Received 27 May 2011; accepted 8 June 2011; published 20 June 2011.

The collision of the Cretaceous Olutorsky Island Arc with eastern Eurasia margin in the northwest Pacific is a critical event in Cenozoic evolution of the Pacific Rim. The timing of synorogenic flysch deposition (Paleocene–Middle Eocene, as young as 45–50 Ma), cross-cutting Shamanka pluton (45 Ma), and an overlap sequence of the Kinkil volcanics (45 Ma) tightly bracket the timing of collision of the far-traveled Olutorsky terrane to the Middle Eocene. This collision may have driven change in plate movement that resulted in the establishment of the Aleutian Arc at this time, which trapped a fragment of the Kula plate (now in the Bering Sea). *KEYWORDS: Kamchatka; Olutorsky Arc; Eocene collision; fission-track and U/Pb dating; zircon; nanoplankton.*

Citation: Soloviev, Alexey V., John I. Garver, Mikhail N. Shapiro, Mark T. Brandon, and Jeremy K. Hourigan (2011), Eocene arc-continent collision in northern Kamchatka, Russian Far East, *Russ. J. Earth. Sci., 12,* ES1004, doi:10.2205/2011ES000504.

Introduction

A major tectonic event in the northwest Pacific was the collision of the Upper Cretaceous Olutorsky terrane (island arc) with the NE Eurasian margin, which was an Andean-style convergent margin at that time [*Bogdanov et al.*, 1990; Geist et al., 1994; *Stavsky et al.*, 1990; *Worrall,* 1991].

The term "Olutorsky terrane" has precedence in the literature [*Bogdanov et al.*, 1990]. This terrane represents mid-Cretaceous to early Tertiary volcanic rocks, oceanic sediments built on oceanic crust. This terrane includes similar rocks referred to as "Olyutorka-Kamchatka island arc terrane" [*Nokleberg et al.*, 1998], "Iruneiskiy island arc terrane" [*Nokleberg et al.*, 1998], "Achaivayamian-Valaginian volcanic arc" [*Shapiro*, 1995].

Remnants of the far-traveled Olutorsky terrane can be traced for almost the entire length of the Kamchatka Peninsula, and likely extend eastward into the Bering Sea as the Shirshov and Bowers Ridge [*Seliverstov,* 1998; *Worrall*, 1991] (Figure 1). Together, these onshore and offshore fragments suggest that this Cretaceous arc may have been as much as 3000 km long but only the part on Kamchatka is exposed for direct observation. Understanding the timing of the collision of the Olutorsky arc with Eurasian continent is crucial to any Cenozoic tectonic reconstruction of northwest Pacific.

The highlight of this Cenozoic collisional suture zone is the spectacular Vatyna-Lesnovsk[1] thrust, which is well exposed in northern Kamchatka (Figure 1). The Vatyna-Lesnovsk thrust is a part of the suture formed during collision of the Cretaceous Olutorsky island arc with Eurasian continental margin. Paleomagnetic data from Cretaceous volcanic rocks (Olutorsky terrane) indicate a paleolatitude of $49.7° \pm 5.6°$N [*Levashova et al.*, 1998], $\sim 20°$ to the south of the expected latitudes for Eurasia and North America ($\sim 70°$N). During the Late Cretaceous to early Tertiary, the Olutorsky arc was transported northward and eventually collided with Eurasian continental margin [*Chekhovich et al.*, 1999; *Geist et al.*, 1994; *Konstantinovskaia*, 2000; *Shapiro*, 1995; *Soloviev et al.*, 1998; *Worrall*, 1991]. The total overthrusting along Vatyna-Lesnovsk suture zone based on simple structural reconstructions and by interpretations of gravity data suggests that there has been at least 50 km [*Bogdanov et al.*, 1990] but may be as much as 100 km [*Soloviev et al.*, 2001].

The timing of the Olutorsky collision has been controversial for years and published estimates for the timing to Olutorsky collision range from the Cretaceous to the Miocene [*Chekhovich et al.*, 1999; *Geist et al.*, 1994; *Konstantinovskaia*, 2000; *Stavsky et al.*, 1990; *Worrall*, 1991]. The

[1]Geological Institute, Russian Academy of Sciences, Moscow, Russia
[2]Geology Department, Union College, Schenectady, New York, USA
[3]Institute of the Physics of the Earth, Russian Academy of Sciences, Moscow, Russia
[4]Department of Geology and Geophysics, Yale University, New Haven, Connecticut, USA
[5]Department of Earth and Planetary Sciences, UC Santa Cruz, Santa Cruz, CA, USA

http://elpub.wdcb.ru/journals/rjes/doi/2011ES000504.html

[1]The northeast and central segments of this fault are referred to as the Vatyna thrust (Koryak Highlands), the Lesnovsk thrust (Lesnovsk Highlands in the Kamchatka Isthmus) respectively.

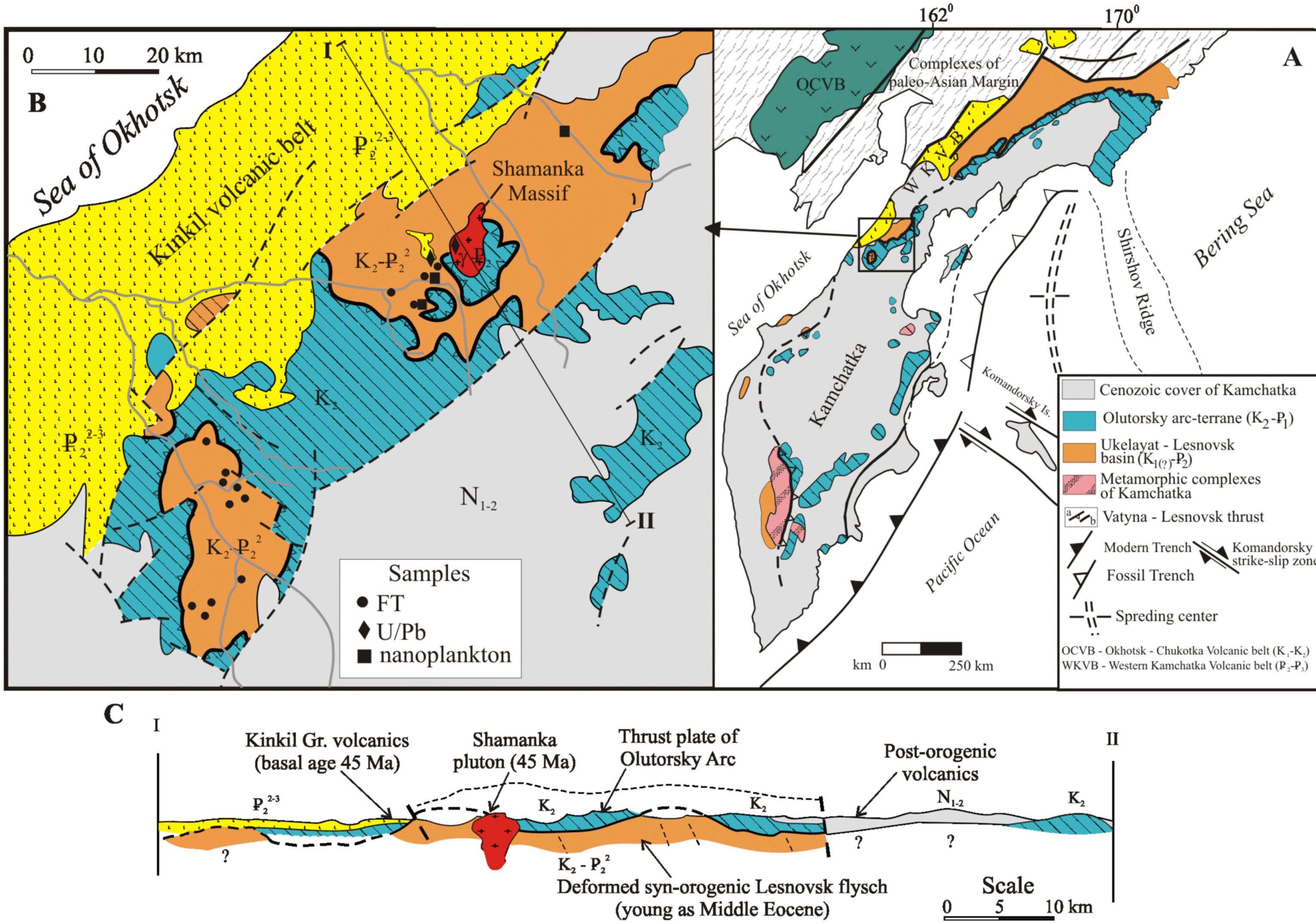

Figure 1. [A] General geological setting Kamchatka (modified from [*Shapiro*, 1995; *Til'man, Bogdanov*, 1992; *Worrall*, 1991]). The Olutorsky arc-terrane lies outboard of Vatyna-Lesnovsk thrust and well exposed in northern Kamchatka. [B] Schematic geologic map showing the geological structure of the Kamchatka Isthmus (left picture) (modified from [*Markovsky*, 1989; *Soloviev et al.*, 2001]). [C] Simplified geological profile cross Lesnovsk Highland.

key to understanding the timing of collision is to constrain the age of rocks caught up in the collisional suture, which is marked by the Vatyna-Lesnovsk thrust. Here, we present new age data for the age of: a) deformed footwall strata below the Vatyna-Lesnovsk thrust; b) stitching intrusions that cut all rocks in the suture zone; and c) neoauthochtonous deposits that unconformably overlie deformed rocks in the collision zone. Taken together, these data tightly bracket the timing of Olutorsky collision. The timing of the collision bears on the evolution of the North Pacific including the establishment of the Aleutian Islands.

Geological Background

The geologic framework of the northwest Pacific includes oceanic and arc terranes of Paleozoic to Cenozoic age that have been accreted to northeast Eurasian margin from the Late Jurassic to Tertiary [*Nokleberg et al.*, 1998; *Stavsky et al.*, 1990]. The Cretaceous Okhotsk-Chukotka volcanic belt (OCVB) is a continental arc built on part of this collage of terranes assembled prior to the Albian. The OCVB is a laterally extensive Andean-style arc that persisted along the southern margin of the western and northern shore Sea of Okhotsk, Bering shelf, and western Alaska [*Filatova,* 1988; *Nokleberg et al.*, 1998; *Tikhomirov et al.*, 2006]. The duration of magmatic activity in OCVB is debated but generally thought to include the Middle Albian to Campanian time [*Filatova*, 1988; *Zonenshain et al.*, 1990]. Arc-related magmatism ceased at $\sim$ 81 Ma within the Okhotsk sector of the OCVB [*Hourigan, Akinin*, 2004]. Following a possible brief hiatus, basaltic lavas with within-plate chemical affinities were erupted over a large part of the belt. $^{40}Ar/^{39}Ar$ data from these volcanic rocks indicate that this latter activity spanned the interval from 78–73 Ma [*Hourigan, Akinin*, 2004]. The OCVB was the source of a thick package of volcanic sediments deposited offshore into the forearc, and these strata are represented by turbidites of the Ukelayat Group in the Koryak Highlands [*Garver et al.*, 2000] and the Lesnovsk Group in the Lesnovsk Highlands in Kamchatka Isthmus (Figure 1).

Fragments of the Upper Cretaceous part of the Olutorsky island arc formed about 2000 km to the south in the Pacific far from the Eurasian continental margin, and the arc activity was inferred to be largely intra-oceanic [*Chekhovich et al.*, 1999; *Levashova et al.*, 1998]. Today, this far-traveled island arc complex has been obducted on to the continental margin and the late thrust that appears to be the suture is the Vatyna-Lesnovsk thrust zone. In this spectacular overthrust, island arc rocks of the Olutorsky terrane sit on a footwall comprised of Cretaceous to Paleogene terrigenous deposits of the Ukelayat basin, which was likely deposited in the forearc region of the OCVB. The Vatyna-Lesnovsk thrust can be mapped as a flat or slightly tilted surface that can be mapped for hundreds of kilometers on northern Kamchtaka (Figure 1) [*Soloviev et al.*, 2001]. In the two areas where we mapped extensively both footwall and hanging wall rocks are exposed but in many part of the Peninsula the structure is buried by younger volcanic rocks of the Kamchatka arc, which was established after collision.

The footwall in the collision zone appears to be comprised almost exclusively of the Cretacoues to Paleocene forearc strata of the Ukelayat basin that contains strata inferred to have been largely derived from the OCVB [*Garver et al.*, 2000]. Based on the age of the youngest strata in the Ukelayat basin, the Olutorsky arc was inferred to collide with Eurasian margin in the Middle Eocene (c. 45–50 Ma) [*Garver et al.*, 2000; *Soloviev et al.*, 1998].

Finally, the collision zone appears to have a significant syn- to early post-collisional suite of volcanic rocks and intrusives that play a key role in bracketing deformation. The Kinkil volcanic belt is located on the northern part of the Western Kamchatka and has also been described as a part of the Western Kamchatka-Koryak volcanic belt (WKKV) (see (Figure 1) (for example, [*Filatova*, 1988]). The collision is inferred to have driven the locus of volcanism eastward to the Kinkil volcanic belt, which includes Upper Eocene to Lower Miocene neoautochthonous deposits that rest unconformably on deformed rocks of the Vatyna-Lesnovsk suture zone. Locally intrusives related to these volcanic rocks are present in the collision zone, and the most notable of these in the Shamanka granite.

Geology of Collision Zone

In the Kamchatka Isthmus area, the low-angle Lesnovsk thrust is well exposed and the underlying deformed rocks of Ukelayat basin are exposed in structural windows along the Vatapvayam dome and the Shamanka dome [*Shantser et al.*, 1985; *Soloviev et al.*, 2001] (Figure 1). Upper plate rocks of the Olutorsky island arc include the Upper Cretaceous MORB and arc-volcanic rocks, pelagic cherts, poorly dated mafic intrusions, and greenschists [*Shantser et al.,* 1985]. The structural thickness of the upper plate is about 2–4 km [*Soloviev et al.*, 2001] (Figure 1). The folds are not typical in the upper plate rocks partly because there is little stratal continuity in these units, but axes of map-scale folds trend northeast-southwest, parallel to the orogenic belt. West-vergent asymmetrical folds in greenschist facies mylonitic rocks occur along faults between the upper plate nappes [*Soloviev et al.*, 2001].

The Ukelayat-Lesnovsk Group is a very thick, deformed turbidite assemblage that makes up the lower plate in the collision zone. A key issue is that the age range of unit has been poorly constrained. The unit is generally composed of poorly fossilliferous medium- to thin-bedded, fine- to medium-grained sandstone and interbedded shale and siltstone. Sandstones are compositionally uniform and are mainly quartzofeldspathic and feldspathic-quartzose graywackes. The composition of sandstones from rocks in northern Kamchatka indicates a source region dominated by a dissected continental arc and paleocurrents indicate largely axial S-to-N sedimentary transport [*Garver et al.*, 2000]. These lower plate rocks are exposed in the center of the two structural domes which appear to have been exhumed

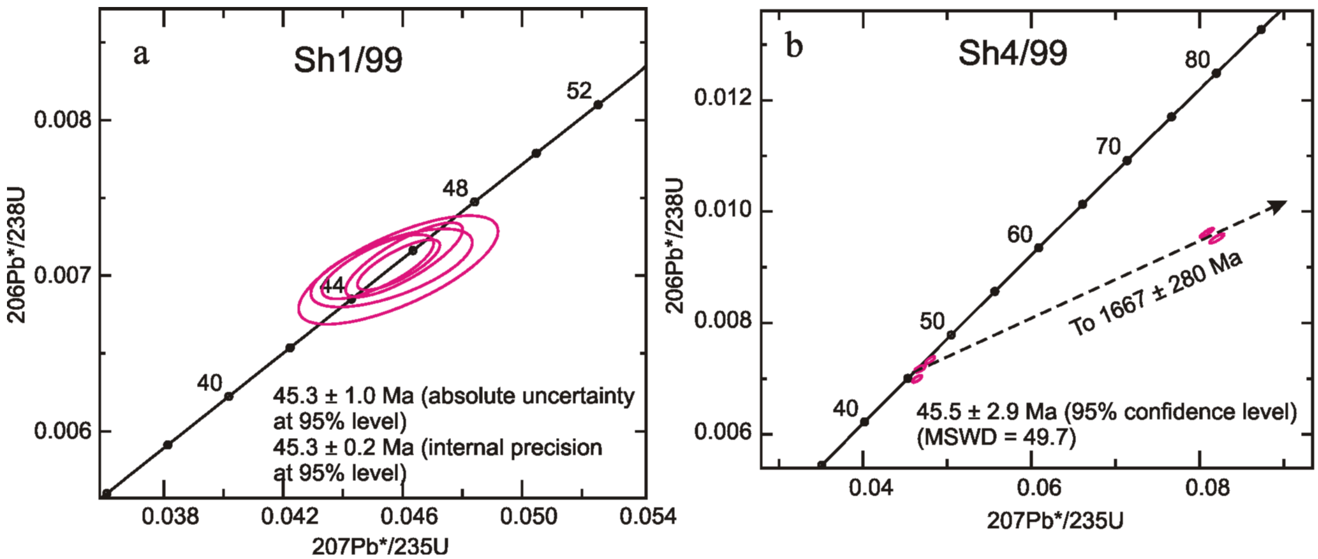

Figure 2. U/Pb isochron diagrams: (a) for the Shamanka granodiorite (sample Sh1/99); (b) for the rhyolites at the base of the Kinkil volcanics(sample Sh4/99).

in the Late Eocene [*Soloviev et al.*, 2002] (Figure 1). These turbidites in the lower plate are dominated by westward-overturned isoclinal folds with north-northeast fold axes that are parallel to the thrust front, which indicate shortening in the direction of thrusting [*Soloviev et al.*, 2001].

The Lesnovsk and Vatyna thrusts were originally interpreted as a stratigraphic contact and thus the turbidites below the upper plate were inferred to older [*Markovsky,* 1989]. As a result of this initial misunderstanding, the turbiditic strata were originally mapped as Cretaceous because the overlying upper plate rocks have a number of mid- to Upper Cretaceous fossils; this simple observation indicated to early workers that the deformed underlying unfossiliferous strata of the Ukelayat were Cretaceous (or older) [*Markovsky*, 1989]. New stratigraphic age constraints presented here and elsewhere include new nanonfossil biostratigraphy and fission-track grain ages on detrital zircon [*Garver et al.*, 2000; *Soloviev et al.*, 2002]. These data indicate that along the thrust front here and to the north, these footwall strata range in age from Upper Cretaceous to Middle Eocene.

Below the frontal thrust zone, large blocks occur enclosed in a chaotic structure and this has been mapped as olistostromal deposits that are the sedimentary record of the collisional process. The matrix in these deformed rocks is composed of mudstones with thin interlayers of fine-grained sandstone that have been pulled apart and tectonically dismembered. Blocks are represented by several lithologies including a distinctive tuff with broken Inoceramus shells, as well as chert, aphyric pillow-basalt, and volcanic sandstone all correlative with upper plate lithology of Vatyna Group (i.e. rocks of the Irunei Group). The ages of chert blocks in the olistostromal deposits and from chert in the Irunei Group in the upper plate are Santonian to Maastrichtian as indicated by radiolaria [*Soloviev et al.*, 2001]. The olistostromal unit represents deformed basin strata with blocks derived from the upper plate that was likely deposited during thrusting, but the age of deposition is not directly constrained. Mass wasting deposits are common in settings where the blocks from upper plate rocks are deposited immediately in front of an advancing thrust sheet and then involved to post-depositional deformations.

The Lesnovsk thrust is well exposed and we evaluated its occurrence and small-scale structures in several places in northern Kamchatka [*Soloviev et al.*, 2001]. The thrust zone is marked by a narrow zone of pervasive brittle deformation commonly less then 100 m thick. The fault zone varies in thickness, and consists of lens-like phacoids with black and green cataclasite with wavy fibered and flaser structure. The thickness of the cataclasite zone varies from 0.5 to 30 meters, but is normally from 5 to 10 meters. Riedel structures in this zone indicate top to the north-northeast transport for thrust in the Vatapvayam Dome area and top to the northwest transport for the thrust in the Shamanka Dome [*Soloviev et al.*, 2001].

Post-orogenic neo-autochthonous strata are well exposed east of the thrust in the isthumus area. These rocks include gently deformed volcanic rocks of Kinkil Group that overlap folded lower plate deposits with an angular unconformity. Rhyolites and their tuffs dominate at the base of the Kinkil Group, but basaltic rocks occur upward in the stratigraphic sequence. Middle to Late Eocene flora from strata of the Kinkil Group have been reported in the literature [*Gladenkov et al.*, 1991] and we determined radiometric ages from several locations (see below).

One of the most crucial relationships that constrain the timing of thrusting occurs in the Kamchatka Isthmus. In this area lower plate rocks are well exposed in a window,

Table 1. U–Pb Isotopic Data and Ages From Shamanka Granodiorite (Sample Sh1/99) and Kinkil Rhyolite (Sample Sh4/99)

Grain type	Grain wt.(μg)	Pb_c (pg)	U (ppm)	$^{206}Pb_m / ^{204}Pb$	$^{206}Pb_c / ^{208}Pb$	Apparent ages (Ma) $^{206}Pb* / ^{238}U$	$^{207}Pb* / ^{235}U$	$^{207}Pb* / ^{206}Pb*$
				Sample Sh1/99				
5A	31	6	241	571	9.6	45.6 ± 1.3	45.7 ± 1.6	51 ± 49
5A	32	11	216	310	5.9	45.3 ± 1.3	45.3 ± 2.2	46 ± 88
5A	29	8	303	502	7.7	45.3 ± 1.1	44.9 ± 1.5	20 ± 55
1Br	11	9	471	283	5.9	45.2 ± 1.8	45.5 ± 2.6	63 ± 99
5Ar	29	9	386	556	3.6	45.4 ± 0.9	45.5 ± 1.1	52 ± 37
				Sample Sh4/99				
5Ar	31	6	1301	3200	21.9	47.1 ± 0.3	$47.6 \pm 0,5$	71 ± 15
5Ar	32	11	3151	4100	20.3	46.1 ± 0.3	46.4 ± 0.5	61 ± 20
5Ar	36	11	1915	2690	20.3	44.9 ± 0.3	46.1 ± 0.5	105 ± 16
5Ar	66	8	1809	9180	13.1	61.7 ± 0.4	78.9 ± 0.6	637 ± 7
5Ar	70	12	1462	5900	19.9	61.1 ± 0.4	80.1 ± 0.7	692 ± 10

$*$ – radiogenic Pb, Grain type: A=$\sim$ 100 μ, B=$\sim$ 200 μ, r = 5 : 1 rod-shaped grain (number of grains analyzed is also shown), $^{206}Pb/^{204}Pb$ is measured ratio, uncorrected for blank, spike, or fractionation, $^{206}Pb/^{208}Pb$ is corrected for blank, spike, and fractionation, Most concentrations have an uncertainty of 25% due to uncertainty in weight of grain, Constants used: $^{238}U/^{235}U = 137.88$. Decay constant for $^{235}U = 9.8485 \times 10^{-10}$, Decay constant for $^{235}U = 1.55125 \times 10^{-10}$. All uncertainties are at the 95% confidence level, Pb blank ranged from 2 to 10 pg, U blank was < 1 pg, Interpreted ages for concordant grains are $^{206}Pb*/^{238}U$ ages if < 1.0 Ga and $^{207}Pb*^{206}Pb*$ ages if > 1.0 Ga. Interpreted ages for discordant grains are projected from 100 Ma. All analyses conducted using conventional isotope dilution and thermal ionization mass spectrometry, as described by [*Gehrels*, 2000].

both lower plate and upper plate rocks are intruded by the Shamanka granite (Figure 1). The pluton has a distinctive contact aureole and the intrusion is accompanied by numerous dikes of basic and felsic composition both of which are cross-cut upper and lower plate rocks. The spatial distribution of dikes has been used to infer that they are related to the effusive rocks of the nearby Kinkil Group [*Shantser et al.*, 1985]. The basal units of the Kinkil Group, which are up to 200–250 m contains pebbles and cobbles of granites, rocks similar to the dikes and hornfels. Flora in these conglomerates of the Kinkil Group is Upper Eocene [*Shantser et al.*, 1985].

New Age Data

We have worked on the overthrust zone in several places in northern Kamchatka [*Soloviev et al.*, 2001]. One area that provides crucial relationships that constrain the timing of thrusting and collision is in the Kamchatka Isthmus. Here we provide the results of new detrital zircon fission track ages (from lower plate sandstones), new determinations of nanoplankton (from mudstones in the lower plate), and previously unreported U/Pb, K/Ar and Rb/Sr ages (Figure 2, Figure 3) on cross-cutting plutonic rocks and their extrusive equivalents (Table 1, Table 2, Table 3).

Table 2. Rb–Sr Isotopic Data and Ages for Shamanka Granodiorite (Sample Sh1/99)

Mineral	Rb, ppm	Sr, ppm	$^{87}Rb/^{87}Sr$	$^{87}Sr/^{86}Sr$	Isochrone age, Ma	Pair minerals	Pair age, Ma	$(^{87}Sr/^{86}Sr)_0$
Plagioclase	6.314	759.0	0.02410± 0.00007	0.70388± 0.00002	44.4 ± 0.1 $(^{87}Sr/^{86}Sr)_0$ =	Plagioclase–hornblende	47.1 ± 1.1	0.70386± 0.00002
Hornblende	9.566	15.86	1.7447± 0.0016	0.70503± 0.00002	0.70389± 0.00003	Plagioclase–biotite	44.37 ± 0.04	0.70386± 0.00002
Biotite	325.4	3.240	295.72± 0.25	0.89023± 0.00003		Biotite–hornblende	44.35 ± 0.04	0.70393± 0.00002

All analyses conducted using isotope dilution with mixed tracer ^{85}Rb–^{84}Sr and mass spectrometry Sector54 (Micromass). The international standard for Sr–SRM987 was used for control. The isotope composition of Sr normalized by $^{86}Sr/^{88}Sr = 0.1194$. Sample was dated by V. N. Golubev (Institute of ore deposit, petrography, mineralogy and geochemistry RAS, Moscow, Russia).

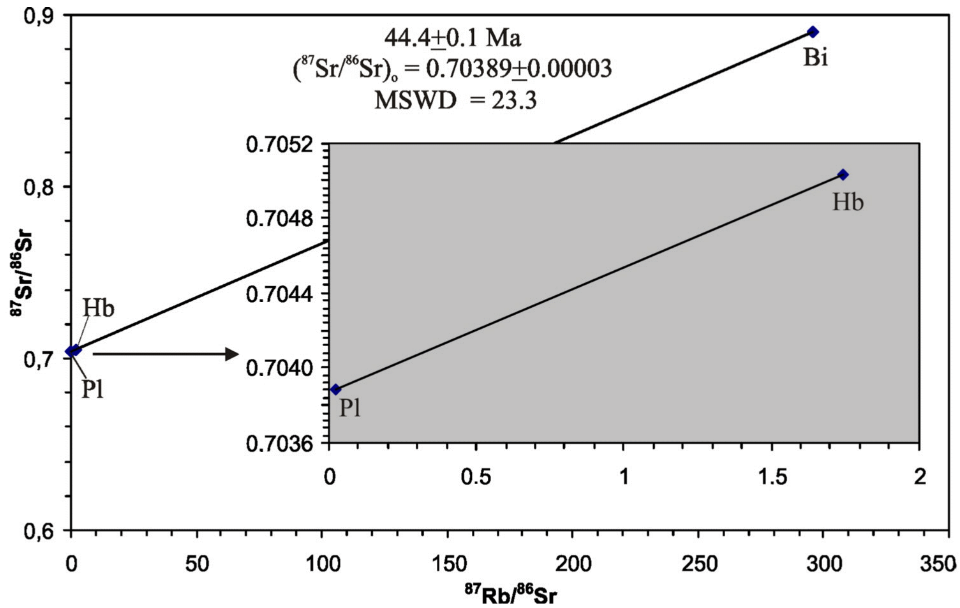

Figure 3. Rb–Sr isochron diagram for the Shamanka granodiorite (sample Sh1/99). Pl – plagioclase, Hb – hornblende, Bi – biotite.

Zircon fission-track data. We collected thirteen new sandstone samples (Table 4) from lower plate deposits for the detrital fission track grain-age analysis (Figure 1), and these data augment our previous data set that has 27 samples [*Garver et al.*, 2000]. Zircon concentrates were prepared using standard methods of separation, and zircons were analyzed using the external detector method [*Bernet, Garver*, 2005; *Garver et al.*, 2000; *Tagami, O'Sullivan*, 2005]. For each sample 45 to 90 zircon grains were counted giving a total of about 1000 single-grain determinations. A binomial peak-fitting method was used to establish principal grain-age components for each sample [*Brandon*, 1996, 2002; *Galbraith, Green*, 1990] (Table 5). This approach requires that maximum temperatures should be $\lesssim 200^\circ$ C to ensure that zircon fission-track ages are primary cooling ages rather than reset during thrusting [*Brandon et al.*, 1998]. Several observations indicate that maximum temperatures of the Ukelayat strata were generally well below ~ 150 or 200°C. The sampled Lesnovsk Group shows only brittle deformation, with no evidence of pressure solution or cleavage formation. FT dating of apatite from the dated zircon samples indicates that detrital apatites are also largely unreset or partially reset and retain old ages that reflect cooling events in the source region (Table 6). From these observations, we conclude that our samples remained well below $\sim 150^\circ$C after deposition (probably $\sim 120^\circ$C or less based on apatite resetting patterns) and therefore the zircon fission-track system has certainly remained closed.

In all samples several age components (or peaks) are present and the different age populations, P1, P2 and P3 (Table 5), represent cooling events in the source-region, either related to near surface magmatism, tectonic exhumation, or erosion [*Bernet, Garver*, 2005; *Brandon, Vance*, 1992; *Garver et al.*, 1999, 2000]. Because we are primarily interested in constraining depositional age we focus on the P1, which defines the minimum grain-age and thus maximum depositional age for each sample [*Bernet, Garver*, 2005; *Brandon, Vance,* 1992; *Carter et al.*, 1995; *Garver et al.*, 1999, 2000; *Kowallis et al.*, 1986]. The youngest population (P1) is composed of from 5 to 50% of the dated grains (Table 5). The P1 component appears to have been derived from active part of a volcanic arc or rapidly exhumed rocks in source

Table 3. K–Ar Data and Ages for Shamanka Granodiorite (Samples Sh1/99) and Kinkil Rhyolite (Sample Sh4/99)

Sample No.	Mineral	K, %, $\pm\sigma$	$^{40}Ar_{rad}$ (ηg/g), $\pm\sigma$	Age, Ma, $\pm 1.6\,\sigma$
Sh1/99	Biotite	6.67 ± 0.06	22.0 ± 0.3	47.0 ± 1.3
Sh1/99	Hornblende	0.54 ± 0.01	1.65 ± 0.06	44.0 ± 2.5
Sh4/99	Biotite	6.75 ± 0.06	21.8 ± 0.3	46.0 ± 1.3

The concentrations of radiogenic ^{40}Ar conducted using isotope dilution with tracer 38Ar and mass spectrometry MI-1201 IG. The concentrations of K determined by flame spectrophotometry. Constants used: $\lambda_k = 0.581 \times 10^{-10} y^{-1}$, $\lambda_{\beta-} = 4.962 \times 10^{-10} y^{-1}$, $^{40}K = 0.01167$ (at. %). Sample was dated by M. M. Arakelyants (Institute of ore deposit, petrography, mineralogy and geochemistry RAS, Moscow, Russia).

Table 4. Locations of the Samples Analyzed by the Geochronological Methods

Field Number	Latitude	Longitude	Elevation, m	Rock type	Unit
Sh1/99	N 59°31′30″	E 161°48′35″	1160	granodiorite	Shamanka massive
Sh2/99	N 59°32′50″	E 161°38′30″	1070	sandstone	Lesnovsk Group
Sh3/99	N 59°31′22″	E 161°39′00″	396	sandstone	Lesnovsk Group
Sh4/99	N 59°33′42″	E 161°35′55″	870	rhyolite	Kinkil volcanics
Sh15/99	N 59°27′57″	E 161°44′43″	1036	sandstone	Lesnovsk Group
Sh21/99	N 59°29′17″	E 161°29′50″	370	sandstone	Lesnovsk Group
L1	N 59°01′46″	E 161°00′35″	874	sandstone	Lesnovsk Group
L2	N 59°02′00″	E 161°04′33″	1197	sandstone	Lesnovsk Group
L4	N 59°00′54″	E 161°02′24″	612	sandstone	Lesnovsk Group
L6	N 59°02′25″	E 160°22′55″	897	monzogabbro	Atvenaivayam M.
L7	N 59°00′45″	E 160°29′50″	691	monzogabbro	Atvenaivayam M.
L9	N 59°11′09″	E 161°11′40″	451	sandstone	Lesnovsk Group
L10	N 59°11′40″	E 161°11′18″	412	sandstone	Lesnovsk Group
L11	N 59°09′57″	E 161°13′00″	936	sandstone	Lesnovsk Group
L12	N 59°10′29″	E 161°13′50″	927	sandstone	Lesnovsk Group
L13	N 59°11′00″	E 161°14′19″	570	sandstone	Lesnovsk Group
L17	N 59°14′05″	E 161°03′10″	180	sandstone	Lesnovsk Group

area. This inference is supported by the fact that volcanic grains are common in the fraction of lithic fragments in the sandstones and many appear to be first-cycle [*Garver et al.*, 2000; *Shapiro et al.*, 2001]. A number of other studies have shown that the FT minimum age can be used as a proxy for depositional age for sandstones derived from active volcanic sources or continental arc terrains [*Bernet, Garver*, 2005]. The young population of grain ages (P1 ages) from this new data set from bedded sandstones span the interval between 58 to 44 Ma, and sample Sh15/99 which was a block, gives

Table 5. Zircon Fission-Track Peak Ages for Lesnovsk Flysch (Northern Kamchatka)

Nsamp.	N_t	Age of the zircon population		
		P1 (Ma)	P2 (Ma)	P3 (Ma)
		Lesnovsk Highland (Shamanka Dome)		
Sh3/99	60	51.6 ± 5.0 (27%)	86.7 ± 8.9 (55%)	131.4 ± 29.2 (18%)
Sh2/99	75	54.1 ± 8.9 (16%)	73.9 ± 13.9 (26%)	132.6 ± 9.2 (58%)
Sh21/99	60	56.1 ± 3.8 (37%)	106.0 ± 11.5 (47%)	150.3 ± 34.2 (16%)
Sh15/99	59	86.1 ± 6.1 (44%)	155.3 ± 11.0 (56%)	–
		Lesnovsk Highland (Vatapvayam Dome)		
L12	67	43.7 ± 3.4 (17%)	70.6 ± 4.4 (67%)	107.0 ± 12.2 (16%)
L1	45	46.0 ± 2.7 (49%)	–	107.3 ± 7.0 (51%)
L9	90	47.0 ± 3.8 (19%)	70.8 ± 5.7 (56%)	104.0 ± 11.9 (25%)
L2	90	48.1 ± 5.0 (7%)	78.1 ± 5.8 (53%)	116.0 ± 8.6 (40%)
L11	90	50.4 ± 5.6 (20%)	70.6 ± 6.6 (65%)	109.7 ± 25.0 (15%)
L10	90	53.9 ± 3.4 (40%)	87.5 ± 6.2 (50%)	176.5 ± 23.8 (10%)
L17	90	54.5 ± 10.4 (5%)	84.6 ± 6.5 (65%)	134.6 ± 18.9 (30%)
L13	89	55.5 ± 3.5 (34%)	93.0 ± 4.8 (66%)	–
L4	90	58.1 ± 4.2 (36%)	83.3 ± 6.3 (51%)	130.5 ± 14.9 (13%)

N_t – number of grains; percentage of grains calculated in a specific peak; Age for each population is in Ma, uncertainties cited at $\pm 1\sigma$. Zircons were dated using standard methods for FT dating using an external detector. Mounts were etched in a NaOH–KOH at 228°C for 15 and 30 hr and then irradiated at Oregon State with a fluence of 2×10^{15} n/cm^2, along with zircon standards and dosimeter CN-5. Tracks were counted on an Olympus BH-P at 1256x, and a ζ-factor of 305.01 ± 6.91 was used. Fission-track ages were computed using the program Zetaage 4.7 [*Brandon*, 1996]. To discriminate the populations by age, we used the program Binomfit 1.8 [*Brandon*, 2002]. Sample treatment is described in [*Bernet, Garver*, 2005; *Garver et al.*, 1999].

=

Table 6. Apatite Fission-Track Data From Lesnovsk Highland

No. Sample	Unit	Elev (m)	ρs	Ns	ρi	Ni	ρd	n	χ^2	Age	$-/+1\sigma$		U±2se	Track length(n)
							Shamanka Dome							
Sh1	Shamanka M.	1160	6.37	187	2.25	660	2.89	15	100.0	42.3	−4.8	+5.4	31.0 ± 2.7	
Sh2	Lesnaya Gr.	1070	3.45	195	0.98	556	2.88	25	0.4	44.6*	−6.7	+7.8	13.6 ± 1.3	
Sh4	Kinkil Gr.	870	4.76	185	1.57	612	2.84	14	99.7	44.3	−5.0	+5.7	22.1 ± 2.0	
							Vatapvayam Dome							
L17	Lesnovsk Gr.	180	5.07	384	1.88	1422	3.22	42	1.8	13.0*	−6.6	+13.4	23.2 ± 1.4	11.72 ± 1.59 (20)
L10	Lesnovsk Gr.	412	3.76	96	1.72	439	3.13	20	38.8	38.4	−4.7	+5.4	21.8 ± 2.2	12.02 ± 1.49 (5)
Ll3	Lesnovsk Gr.	570	3.44	150	1.32	574	3.20	28	1.4	40.9*	−4.9	+5.6	16.4 ± 1.5	12.52 ± 2.00 (14)
L4	Lesnovsk Gr.	612	6.84	247	2.07	747	3.04	22	69.2	56.3	−5.4	+5.9	27.1 ± 2.2	11.70 ± 1.49 (19)
L1	Lesnovsk Gr.	874	5.57	340	1.61	982	3.00	45	5.1	58.2	−5.2	+5.7	21.3 ± 1.5	11.65 ± 1.17 (21)
L12	Lesnovsk Gr.	927	5.66	246	1.53	667	3.18	28	62.8	65.6	−6.3	+7.0	19.2 ± 1.6	11.70 ± 1.32 (21)
L11	Lesnovsk Gr.	936	2.48	554	0.98	2189	3.15	89	0.0	40.6*	−3.6	+3.9	12.4 ± 0.6	11.81 ± 1.61 (60)
L2	Lesnovsk Gr.	1197	3.90	178	1.82	831	3.02	17	22.4	36.3	−3.7	+4.1	24.0 ± 1.8	12.35 ± 1.46 (11)
							Gabbro in ultramafic massif (upper plate rock)							
L6	Atvenaivayam M.	897	6.80	406	1.75	1043	3.06	30	76.2	66.6	−5.7	+6.3	22.7 ± 1.6	13.32 ± 1.35 (55)
L7	Atvenaivayam M.	691	6.77	475	1.48	1038	3.09	30	100.0	79.0	−6.6	+7.2	19.1 ± 1.3	13.12 ± 1.34 (52)

In this table ρs is the density (cm^{-2}) of spontaneous tracks ($\times 10^5$) and Ns is the number of spontaneous tracks counted; ρi is the density (cm^{-2}) of induced tracks ($\times 10^6$); and ρd is the density (cm^{-2}) of tracks on the fluence monitor ($\times 10^6$); n is the number of grains counted; and χ^2 is the Chi squared probability in percent. Apatite fission track ages ($\pm 1\sigma$ were calculated using the Zeta method, and ages were calculated using the computer program and equations in Brandon (1992). The Zeta factor (for L1–L17 samples) of 112.49 ± 7.53 (± 1 se) is based on forth Zeta determinations from both the Fish Canyon Tuff and the Durango apatite (for Sh1–Sh21 – 103.73 ± 8.77 is based on 3 Zeta determination). All ages that pass χ^2 ($> 5\%$) are reported as pooled ages, otherwise mean ages are shown. Glass (CN-1) monitors, placed at the top and bottom of all irradiation packages (for Zeta Calculations) were used to determine the fluence gradient in each package. All samples were counted and track lengths were measured at 1562.5x using a dry 100x objective (12.5 oculars and 1.25x multiplication factor) on an Olympus BH-2 microscope (for L1–L17 samples) and 1600x using a dry 100x objective (10 oculars and 1.6x multiplication factor) on Olympus BX60 microscope (for Sh1–Sh21 samples) fitted with an automated stage and a Calcomp digitizing tablet. Calibration for track length measurements (given as mean track length, standard deviation, and number measured) was accomplished by repeatedly measuring 20 μm increments on a graticule prior to actual measurements on these samples.

* – BinomFit ages [*Brandon*, 2002] ($\chi^2 < 5\%$); χ^2 ($> 5\%$) – pooled ages.

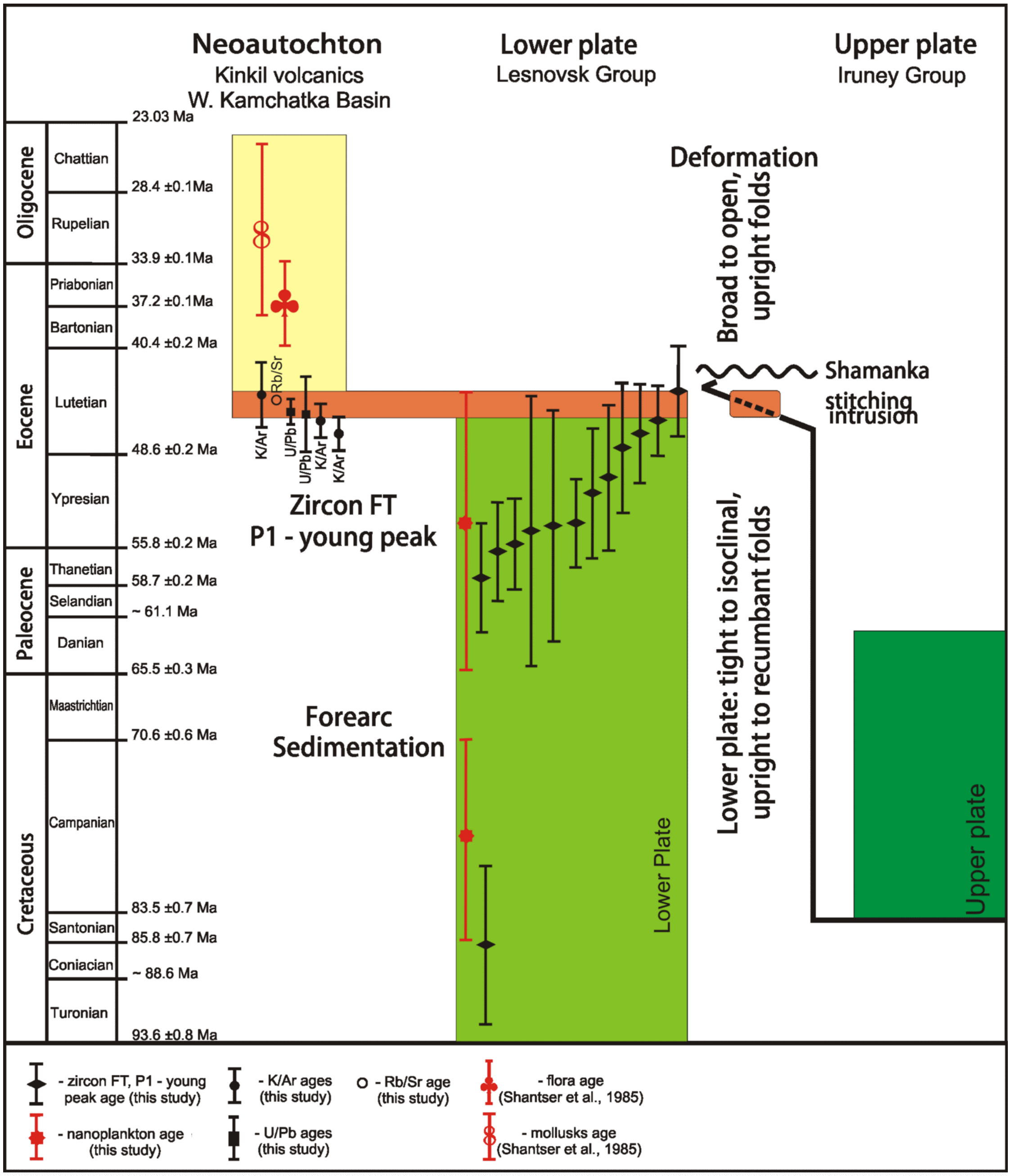

Figure 4. Isotopic and biostratigraphic data from lower plate of Olutorsky collision zone and from neoautochthonous complex in the northern Kamchatka: implication for collision of Olutorsky Arc with Eurasian continental margin. The stratigraphic chart is by [*Ogg et al.*, 2008].

a P1 age of 86.1 ± 6.1 Ma (Table 5, Figure 4). These compare to the age range of 88 to 44 Ma from our other data set (see [*Garver et al.*, 2000]). Together, these ages are remarkable given the fact that the sampled units of bedded sandstone and shale were all previously mapped as Cretaceous, as discussed above: our results show that most are Paleocene. The new samples that we report here come entirely from the footwall of the Vatyna-Lesnovsk suture. We infer that the P1 ages are maximum ages for the deposition of the units, and that overthrusting must be younger than the age of these sandstones. However, we suspect that there may be very short time separating deposition of the sandstones and overthrusting. P1 was probably derived, at least in part, from a contemporaneous volcanic source, because the young population is made of colorless euhedral zircon grains. In addition, U/Pb ages of grains from Ukelayat sandstones show that some grains are the same age as P1 [*Hourigan et al.*, 2009; *Reiners et al.*, 2005]. As discussed, the Ukelayat-Lesnovsk flysch contains olistostomes inferred to be mass wasting deposits that are evidence of syncolli-

=

Table 7. Nanoplankton from the Lesnovsk Group (Lesnovsk Highland, Northern Kamchatka)

Nannoplankton species	Number of Sample																	
	902-1	9902-5	9902-7	9902-11	9902-20	9903-4	9903-5	9903-6	9903-11	9903-15	9903-16	9903-18	9904-7	9906-7	9911-7	9911-8	9911-12	9911-17
Cyclicargolithus floridanus					■		■		■									
Coccolithus pelagicus								■			■							
Sphenolithus primus/moriformis	■			■		■					■			■				
Dictyococcites bisectus									■			■						
Reticulofenestra umbilicus									■	■								
R. haqii									■									
R. dictyoda													■					
Helicosphaera compacta					■													
Chiasmolithus cf. Nitidus									■									
Zyghablithus bijugatus						■												
Micula decussata			■															
Neochiastozygus sp.		■																
Thoracosphaera sp.									■									
Watznaueria barnesae	■															■	■	■
Reinchardtites anthiphorus															■			
Eiffellithus turriseffeli																	■	

Mudstones were collected in Shamanka Dome area. The nanoplankton were identified by E. A. Shcherbinina (Geological Institute of RAS, Moscow).

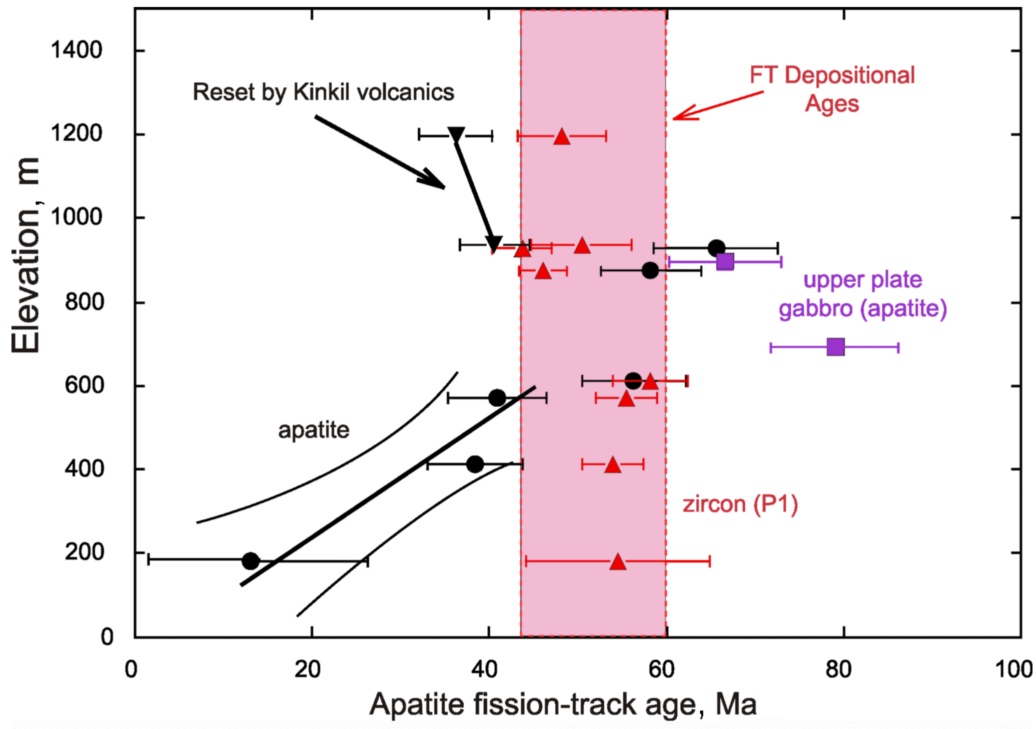

Figure 5. Age-elevation relationship of fission-track data from the Lesnovsk Highland. FT depositional ages (P1) of zircon shown in red. These ages define a depositional interval (pink) of Middle Eocene and older. Apatite ages indicate slow post-orogenic exhumation and possibly post-orogenic heating from the top by the Kinkil volcanics.

sional deposition. Our conclusion is that the youngest of the P1 ages, which are Middle Eocene, are nearly synchronous with collision: the other P1 ages are precollisional and likely represent a long interval of deposition in the forearc basin that was outboard of the OCVB.

Nanoplankton. We collected mudstones from the same sequence that we took sandstones for ZFT analysis for biostratigraphic analysis. Nanoplankton from 18 samples (Table 7) from the upper part of the Lesnovsk Group yield Paleocene through Middle Eocene assemblages and these new ages closely correspond to the age of P1 zircons from sandstones [*Soloviev et al.*, 2002]. Together these ages, obtained independently from a number of sites using different methods, now indicate with certainty that the upper part of the Ukelayat-Lesnovsk flysch is largely if not entirely Eocene in age (Figure 4).

U/Pb age on zircon. To further refine our age control, we collected one sample from the granitic rocks of the Shamanka massif (Table 4, Figure 1) and one from the Kinkil volcanics and dated them by several different methods (Table 1, Table 2, Table 3, Table 4, Figure 1, Figure 2, Figure 3). A new U/Pb age on zircon from the Shamanka Massif is 45.3 ± 1.0 Ma (95% CI), sample Sh1/99 (Table 1, Figure 2). The Kinkil volcanics, which are inferred to be comagmatic with the Shamanka, give a U/Pb age on zircon of 45.5 ± 2.9 Ma (95% CI) (Table 1, Figure 2). from a sample from the basal member.

The overthrust zone is intruded by the Shamanka granitic massif, and the deformed Lesnovsk Flysch is unconformably overlain by the volcanics of Kinkil Group (Figure 1). The end of collision must be marked by intrusion of the Shamanka granites into the overthrust zone because the intrusion cuts both upper plate and lower plate rocks. Previous studies have demonstrated that sandstones and siltstones bearing Upper Eocene to Lower Oligocene mollusks are stratigraphically correlative to the Kinkil Group. Neoautochthonous strata contain basal conglomerates with pebbles derived from the Shamanka pluton. An Upper Eocene fossil flora [*Shantser et al.*, 1985] occurs within the conglomeratic strata.

Post-Orogenic Cooling

The Middle–Upper Eocene Kinkil Volcanics rest unconformably on Lesnovsk suture zone and they are slightly tilted. The Neogene volcanics are horizontal. The fission-track ages from detrital apatite indicate partial resetting (Table 6), so collisional burial of lower plate flysch was less than $\sim$ 4 km. The age-elevation relationship (Figure 5) indicates very slow post orogenic exhumation, less than 50 m/Myr. The partial resetting of apatite at high elevations (see Table 6, Figure 5) may reflect heating by the Kinkil volcanics which unconformably blanketed the structural dome immediately after collision at $\sim$ 45 Ma.

Conclusions

Detrital zircon FT grain-age data in concert with nanoplankton biostratigraphic data suggest that part of the Ukelayat-Lesnovsk Group comprises principally Paleocene to Middle Eocene strata. The end of deposition of the lower plate sediments, deformation, and the subsequent onset of magmatism recorded in Kinkil Group occurred at c. 45 Ma (Middle Eocene). These data allow us to propose that thrusting driven by collision of the Olutorsky island-arc with northeastern Asia took place at about 45 Ma, perhaps over a short period of time ($\sim$ 1 Myr).

D. M. Worrall [1991] proposed that the Olutorsky arc collided with Eurasia at about 56 Ma and this collision, with its attendant changes in slab-pull stress on Kula plate, may have been the underlying cause of change in plate motion. Our data suggest that the collision of the Olutorsky arc with Eurasia happened at 45 Ma and we speculate that this collision may have driven Pacific plate reconstruction at 43 Ma [*Engebretson et al.*, 1985]. As such, if the Olutorsky terrane continues offshore into the Bowers and Shirshov ridges in the Bering Sea [*Worrall,* 1991], then it is likely that the development of the Aleutian Ridge post-dated collision at 45 Ma. In this case, older ages reported from the Aleutians may not represent early onset of the Aleutian Arc, but rather older rocks that were somehow brought into the vicinity of the modern arc.

Acknowledgments. This study was supported by the grant of the President of the Russian Federation MD-1053.2010.5 (to Soloviev), by the Federal Targeted Research Program "Leading Scientific Schools" (SS-7091.2010.5), by the Program for Basic Research of the Division of Earth Sciences, Russian Academy of Sciences, no. 4 and no. 6. This work also was funded by the National Science Foundation (9418990 to Brandon, 9418989 to Garver), the Union College Faculty Development Fund (Garver/Soloviev). We are grateful to G. E. Gehrels for U/Pb dating, M. M. Arakelyants for K/Ar dating, V. N. Golubev for Rb/Sr dating, E. A. Shcherbinina for nanoplankton determinations. Thanks are due to all the workers of the Kamchatka Geological Survey Expedition whose logistical support enabled us to carry out this work. Irradiation of the samples was assisted by the U.S. DOE Reactor Use Sharing program awarded to the Oregon State nuclear reactor (USA).

References

Bernet, M., J. I. Garver (2005), Fission-track analysis of detrital zircon. Low-Temperature thermochronology, *Reviews in Mineralogy and Geochemistry, Reiners P. W. and Ehlers T. (Eds.), 58*, 205–238.

Bogdanov, N. A., S. M. Til'man, V. D. Chekhovich (1990), Late Cretaceous-Cenozoic history of the Koryak-Kamchatka region and the Commander basin of the Bering Sea, *International Geological Review, 32*, 1185–1201, doi:10.1080/00206819009465850.

Brandon, M. T. (1996), Probability density plot for fission-track grain-age samples, *Radiation Measurements, 26*, 5, 663–676, doi:10.1016/S1350-4487(97)82880-6.

Brandon, M. T. (2002), Decomposition of mixed grain-age distributions using BINOMFIT, *On Track, 24*, 13–18.

Brandon, M. T., J. A. Vance (1992), Fission track ages for detrital zircon grains: implication for tectonic evolution of the Cenozoic Olympic subduction complex, *American Journal of Science, 292,* 565–636, doi:10.2475/ajs.292.8.565.

Brandon, M. T., M. K. Roden-Tice, J. I. Garver (1998), Late Cenozoic exhumation of the Cascadia accretionary wedge in the Olympic Mountains, northwest Washington State, *Geological Society of America Bulletin, 110*, 985–1009, doi:10.1130/0016-7606(1998)110<0985:LCEOTC>2.3.CO;2.

Carter, A., C. Bristow, A. J. Hurford (1995), The application of FT analysis to the dating of barren sequences: examples from red beds in Scotland and Tialand, *Non-biostratigraphic methods of dating and correlation. Geological Society [London] Special Publication, Dunay R. E., Hailwood E. A. (Eds.), 89*, 57–68.

Chekhovich, V. D., D. V. Kovalenko, G. V.Ledneva (1999), Cenozoic history of the Bering Sea and its northwestern margin, *Island Arc, 8*, 168–180, doi:10.1046/j.1440-1738.1999.00229.x.

Engebretson, D. C., A. Cox, R. G. Gordon (1985), Relative motions between oceanic and continental plates in the Pacific Basin, *Geological Society of America Special Paper, 206*, 59.

Filatova, N. I. (1988), *Peri-Oceanic Volcanic Belts* (In Russian), Nedra, Moscow, 262.

Galbraith, R. F., P. F. Green (1990), Estimating the component ages in a finite mixture, *Nuclear Tracks and Radiation Measurements, 17*, 197–206, doi:10.1016/1359-0189(90)90035-V.

Garver, J. I., M. T. Brandon, M. Roden-Tice, P. J. J. Kamp (1999), Exhumation history of orogenic highlands determined by detrital fission-track thermochronology, *Exhumation Processes: Normal Faulting, Ductile Flow and Erosion, Ring, U., et al. (Eds.), Geological Society [London] Special Publications, 154,* 283–304.

Garver, J. I., A. V. Soloviev, M. E. Bullen, M. T. Brandon (2000), Towards a more complete records of magmatism and exhumation in continental arcs, using detrital fission-track thermochronometry, *Physics and Chemistry of the Earth, Part A, 25*, 6–7, 565–570.

Geist, E. I., T. L. Vallier, D. W. Scholl (1994), Origin, transport and emplacement of an exotic island-arc terrane exposed in eastern Kamchatka, Russia, *Geological Society of America Bulletin, 106*, 1182–1194, doi:10.1130/0016-7606(1994)106<1182:OTAEOA>2.3.CO;2.

Gehrels, G. E. (2000), Introduction to detrital zircon studies of Paleozoic and Triassic strata in western Nevada and northern California, Paleozoic and Triassic paleogeography and tectonics of western Nevada and northern California, *Geological Society of America Special Paper, Soreghan M. J., Gehrels G. E. (Eds.), 347*, 1–18.

Gladenkov, Yu. B., (1991), *The Eocene of Western Kamchatka* (In Russian), Nauka, Moscow, 181.

Hourigan, J. H., V. V. Akinin (2004), Tectonic and chronostratigraphic implications of new 40Ar/39Ar geochronology and geochemistry of the Arman and Maltan-Ola volcanic fields, Okhotsk-Chukotka volcanic belt, northeastern Russia, *GSA Bull., 116*, 5/6, 637–654, doi:10.1130/B25340.1.

Hourigan, J. K., M. T. Brandon, A. V. Soloviev, A. B. Kirmasov, J. I. Garver, J. Stevenson, P. W. Reiners (2009), Eocene arc-continent collision and crustal consolidation in Kamchatka, Russian Far East, *American Journal of Science, 309*, 333–396, doi:10.2475/05.2009.01.

Konstantinovskaia, E. A. (2000), Geodynamics of an Early Eocene arccontinent collision reconstructed from the Kamchatka Orogenic Belt, NE Russia, *Tectonophysics, 325*, 87–105, doi:10.1016/S0040-1951(00)00132-3.

Kowallis, B. J., J. S. Heaton, K. Bringhurst (1986), Fission-track dating of volcanically derived sedimentary rocks, *Geology, 14*, 19–22, doi:10.1130/0091-7613(1986)14<19:FDOVDS>2.0.CO;2.

Levashova, N. M., M. N. Shapiro, M. L. Bazhenov (1998), Late Cretaceous paleomagnetic data from the Median Range of Kamchatka, Russia; tectonic implications, *Earth and Planet. Sci. Lett., 163*, 235–246, doi:10.1016/S0012-821X(98)00190-3.

Markovsky, B. A. (1989), *Geological map of the USSR, Scale 1:1,000,000 (New series), Quadrangle P-(57, 58), Palana, Explanatory note* (In Russian), VSEGEI, Leningrad.

Nokleberg, W. J., L. M. Parfenov, J. W. H. Monger, I. O. Norton, A. I. Khanchuk, D. B. Stone, D. W. Scholl, K. Fujita (1998), Phanerozoic tectonic evolution of the circum-north Pacific, *U.S. Geological Survey Open File Report, 98-754*.

Ogg, J. G., G. Ogg, F. M. Gradstein (2008), *The Concise Geologic Time Scale*, Cambridge, New York, Melbourne, Cambridge University Press, 177.

Reiners, P. W., I. H. Campbell, S. Nicolescu, C. M. Allen, J. K. Hourigan, J. I. Garver, J. M. Mattinson, D. S. Cowan (2005), (U-Th)/(He-Pb) double dating of detrital zircons, *American Journal of Science, 305*, 259–311, doi:10.2475/ajs.305.4.259.

Seliverstov, N. I. (1998), Evolution of a junction zone between the Kuril-Kamchatka and Aleutian island arcs; a geodynamic model, *Volcanology and Seismology, 19,* 269–275.

Shantser, A. E., M. N. Shapiro, A. I. Koloskov, A. I. Chelebaeva, V. N. Sinel'nikova (1985), Evolution of the structure of the Lesnaya upland and adjoining territories in Cenozoic (north Kamchatka) (In Russian), *Geology of Pacific Ocean, 4,* 66–74.

Shapiro, M. N. (1995), The Upper Cretaceous Achaivayamian-Valaginian volcanic arc and kinematics of the North Pacific plates, *Geotectonics, 29*, 1, 52–64.

Shapiro, M. N., A. V. Soloviev, J. I. Garver, M. T. Brandon (2001), Sources of zircons from Cretaceous and lower Paleogene terrigenous sequences from the southern Koryak upland and western Kamchatka, *Lithology and Mineral Resources, 36*, 322–336, doi:10.1023/A:1010458120285.

Soloviev, A. V., M. T. Brandon, J. I. Garver, M. N. Shapiro, G. V. Ledneva (1998), Collision of the Olutorsky Island Arc with Eurasian continental margin: kinematic and age aspects, *Doklady Earth Science, 361,* 5, 632–534.

Soloviev, A. V., M. T. Brandon, J. I. Garver, M. N. Shapiro (2001), Kinematics of the Vatyn-Lesnaya thrust fault (Southern Koryakia), *Geotectonics, 35*, 6, 471–489.

Soloviev, A. V., M. N. Shapiro, J. I. Garver, E. A. Shcherbinina, I. R. Kravchenko-Berezhnoy (2002), New age data from the Lesnaya Group: A key to understanding the timing of arc-continent collision, Kamchatka, Russia, *The Island Arc, 11*, 1, 79–90, doi:10.1046/j.1440-1738.2002.00353.x.

Stavsky, A. P., V. D. Chekhovich, M. V. Kononov, L. P. Zonenshain (1990), Plate tectonics and palinspastic reconstruction of the Anadyr-Koryak region, northeast USSR, *Tectonics, 9,* 81–101, doi:10.1029/TC009i001p00081.

Tagami, T., P. B. O'Sullivan (2005), Fundamentals of fission-track thermochronology, Low-Temperature thermochronology, *Reviews in Mineralogy and Geochemistry, Reiners P. W., Ehlers T. (Eds.), 58*, 19–47.

Tikhomirov, P. L., V. V. Akinin, V. O. Ispolatov, P. Alexander, I. Yu. Cherepanova, V. V. Zagoskin (2006), The Okhotsk-Chukotka volcanic belt: Age of its northern part according to new Ar–Ar and U–Pb geochronological data, *Stratigraphy and Geological Correlation, 14*, 5, 524–537, doi:10.1134/S0869593806050054.

Til'man, S. M., N. A. Bogdanov (1992), *Tectonic map of northeast Asia: Institute of the Lithosphere, Russian Academy of Sciences and Circum-Pacific Council for Energy and Mineral Resources, 1: 5,000,000 scale map,* Moscow, Russia, 29.

Worrall, D. M. (1991), Tectonic history of the Bering Sea and evolution of Tertiary strike-slip basins on the Bering shelf, *Geological Society of America Special Paper, 257*, 120.

Zonenshain, L. P., M. I. Kuzmin, L. M. Natapov, B. M. Page (1990), Geology of the USSR: a plate-tectonic synthesis, *American Geophysical Union, Geodynamics Series, 21*, 242.

Mark T. Brandon, Department of Geology and Geophysics, Yale University, New Haven, Connecticut, USA.

John I. Garver, Geology Department, Union College, Schenectady, New York, USA.

Jeremy K. Hourigan, Department of Earth and Planetary Sciences, UC Santa Cruz, Santa Cruz, CA, USA.

Mikhail N. Shapiro, Institute of the Physics of the Earth, Russian Academy of Sciences, Moscow, Russia.

Alexey V. Soloviev, Geological Institute, Russian Academy of Sciences, Moscow, Russia.